Journal of Thermal Analysis and Calorimetry, Vol. 63 (2001) 31–46

THE ADSORPTION AND CURING BEHAVIORS OF THE EPOXY/AMIDOAMINE SYSTEM IN THE PRESENCE OF METAL OXIDES

S.-G. Hong and J.-S. Tsai

Department of Chemical Engineering, Yuan-Ze University, Chung-Li, Tao-Yuan 320, Taiwan

(Received January 19, 2000; in revised form June 19, 2000)

Abstract

The curing and adsorption behaviors of an epoxy/amidoamine system under the influence of iron, aluminum, and zinc oxides are studied by using differential scanning calorimetry (DSC) and diffuse reflectance infrared spectroscopy (DRIFT). From DRIFT, it is obtained that the amidoamine curing agent is preferentially adsorbed on the three metal oxide surfaces. The amount of amidoamine adsorbed is in the order of iron oxide>zinc oxide>aluminum oxide. Moreover, the iron and zinc oxides adsorb resins more firmly than the aluminum oxide. The results of DSC analyses indicate that more amine related exotherms are found in the specimen filled with the iron oxide but more amide related exotherms are found in the zinc oxide added specimens and they are related to the difference in the preferential adsorption found on three metal oxides. The curing characteristics are also changed in the presence of metallic fillers and the greatest change is obtained from the specimen containing the iron oxide.

Keywords: curing, DRIFT, DSC, epoxy, metal oxide, preferential adsorption

Introduction

Due to the great versatility of epoxy resins, numerous epoxy systems used as coatings or bonding materials for the metal substrates have been formulated. It is well recognized that the interfacial compositions of resin/substrate bonding systems play an important role in determining the durability of the adhesive bonds. The adhesive interphase usually shows a distinct chemical composition and has properties different from those in the bulk resin [1]. Many studies have been done on analyzing the interfacial reactions of different epoxy/metal systems [1–4].

Nigro and Ishida showed that the extents of the epoxide consumption and the ether formation increased with decreasing the coating thickness of the epoxy film on the steel surface [2]. This was attributed to the surface effect of the steel, which led to a high conversion of the epoxy resin near the steel surface. A similar behavior was found on the copper surface [3]. Dillingham and Boerio also indicated that the amine curing agent was protonated by acidic hydroxyl groups in the aluminum hydroxide

1418–2874/2001/ $ 5.00

Akadémiai Kiadó, Budapest
Kluwer Academic Publishers, Dordrecht

[5]. Furthermore, the hydroxyl groups could catalyze the curing reaction and form an adhesive layer with a higher degree of crosslinks close to the oxide surface. However, an incomplete curing of the epoxy adhesive near the aluminum surface was reported by Kollek and Brockmann [4].

Carter *et al.* studied the reactions of an epoxy-dicyandiamide (DICY) system with the cold rolled steel (CRS) and electrogalvanized steel (EGS) surfaces, and found a new compound generated due to the specific chemical reaction between DICY and the EGS [6]. DICY was reduced when heated with metallic zinc at 170°C for a short time, whereas no reaction was observed when heated against steel or zinc oxide [6, 7]. In spite of the zinc and steel, DICY could form guanylurea upon heating on an anodic aluminum oxide surface [8].

Regarding the effect on the curing reaction, it was reported that the zinc filler was capable of changing the curing activation energy of the epoxy resin [9]. The catalytic effect was also obtained from the epoxy system with aluminum oxide added as the filler [10]. It was shown previously that the presence of Fe_2O_3, ZnO, and $Al(OH)_3$ fillers increased the initial curing speed of the epoxy/DICY but decreased the glass transition temperature [11]. A similar result was obtained from other epoxy systems [10, 12].

Despite these reactions, the metal surface could show various degrees of preferential adsorption of the specific constituent from the epoxy system in contact. In general, the preferential adsorption was metal dependent and could result in an interfacial layer that had a reduced crosslinking density and a low cohesive strength adjacent to the metal surface [1, 13, 14]. As a result, the chemistry of the resin near the metal surface and the stability of the boundary layer were affected.

It was shown that the preferential adsorption of amino groups from the epoxy/polyamide system occurred on the electrogalvanized steel (EGS) surface during cure [15]. In addition, the extent of cure of the epoxy/polyamide near the EGS surface was affected by these abundant amino groups. Yet the similar phenomenon was not obtained when the same adhesive was cured on a cold-rolled steel surface (CRS) [16]. The attraction of polyamide curing agent to the surfaces of aluminum and iron oxides was reported earlier by Baldwin *et al.* [17]. Hong also confirmed with reflection absorption infrared spectroscopy that the amount of polyamide adsorbed on the metal substrates followed the order of Cu>Fe>Al [18].

In the case of other curing agents, Nakamae *et al.* showed that the aromatic amine curing agent could be selectively adsorbed onto the aluminum oxide [19]. A large amount of amine curing agent was also found to be present on the copper surface [20]. Additionally, Boerio and Hong indicated that DICY curing agent was adsorbed from the epoxy/DICY onto the silver surface to form an interface that was abundant in DICY [21]. In the previous study, it was concluded that a significant amount of unreacted DICY was present on the CuO and Cu_2O surfaces [22]. The adsorption of the curing agent onto the solid surface during cure was frequently observed [23].

In this study, the adsorption and curing behaviors of the epoxy/amidoamine system filled with different metal oxides are studied with diffuse reflectance infrared

spectroscopy (DRIFT) and differential scanning calorimetry, respectively. It is shown that the results from these two analyses are complementary to each other and consistently describe the effect of the adsorption on the curing reaction of the epoxy system.

Experimental

Material

The epoxy resin was Epon 828 from Shell Chem. Co. with the epoxy equivalent mass near 190. The amidoamine curing agent was Weldmide 3220 from Weldon Chem. Co. with an active hydrogen equivalent mass about 200. The metallic fillers, iron oxide (Fe_2O_3, purity= 99.8%, diameter=100 micrometers), zinc oxide (ZnO, purity= 99.9%, diameter=120 micrometers), and aluminum oxide (Al_2O_3, purity= 99.0%, diameter=120 micrometers) were from Tokyo Kasei Chem. Co.

DRIFT analysis

Firstly, the metal oxides were immersed in the tetrahydrofuran (THF) solutions containing 0.05, 0.2, and 1 mass% of the epoxy/polyamide mixtures at 30°C for an hour. In a separate test, the epoxy/polyamide mixture with no THF solvent was also prepared. Then the metal oxides were centrifuged from the solutions, rinsed with the fresh THF solvent, and subsequently cured at 80°C for 3 h. The treated metal oxides (1 mass%) were mixed with KBr powders and then placed in the DRIFT accessory (EasiDiff from Pike Technologies) to obtain DRIFT spectra of the adsorbed layers. Two hundred scans were acquired at a resolution of 4 cm^{-1} from 4000 to 1000 cm^{-1} on a Nicolet 550 Fourier transform infrared spectrophotometer equipped with the MCT detector. Difference spectra were obtained by subtracting the baseline spectrum of the KBr powder mixed with the uncoated oxide.

Table 1 The compositions of the DSC specimens

Specimen	Epoxy	Amidoamine	Fe_2O_3	Al_2O_3	ZnO
D1	100	105	0	0	0
D2	100	105	5	0	0
D3	100	105	0	5	0
D4	100	105	0	0	5

(Relative mass based on 100 parts epoxy resin)

DSC analysis

The compositions of specimens tested are listed in Table 1. The specimens are formulated in the stoichiometric balance of the curing agent and the epoxy. In preparing specimens, the epoxy resin and the metal oxide were weighed and mixed in a Retsch centrifugal ball mill (model SI) for 30 min before the curing agent was added. The

curing exotherm was obtained by dynamic scanning (2°C and 10°C min^{-1}) the hermetic specimens in a Perkin Elmer DSC-7 under nitrogen environment (with a nitrogen flow rate of 30 ml min^{-1}). The homogeneity of the specimens prepared was confirmed by the small standard deviations obtained from the DSC curing exotherms.

The curve-fitting of the DSC exotherms follows the procedures listed below:

1. Firstly, using the exotherm obtained at a scanning rate of 2°C min^{-1}, the peak positions of the two overlapped exotherms are determined by taking the second derivative of the original exotherm. The background is assumed to be a horizontal line and removed.
2. The full width half maximum (FWHM) and the curve shape are determined by curving fitting the left side of the exotherm because it is the place that is less affected by the other adjacent peak. Once the FWHM and the curve shape (which is 85% Gaussian and 15% Lorenzian in this case) are settled, the other peak at the position determined previously is added.
3. The intensities of two curves are adjusted to get the best fit.
4. The FWHM and the peak shape are kept constant for other specimens tested at the same scanning rate.
5. Regarding the exotherms obtained at a scanning rate of 10°C min^{-1}, the peak positions of the overlapped exotherms are determined by using the peak positions obtained from the exotherms at a scanning rate of 2°C min^{-1} (i. e., from the procedure (1)) and the method proposed by Kissinger to minimize the curve-fitting artifact [24]. Then the same procedures as shown in (2~4) are followed.

Results and discussion

DRIFT analyses

The representative DRIFT spectra taken from the iron oxide coated in solutions containing different concentrations of epoxy system are shown in Fig. 1. In Fig. 1A, the large bands near 2924 and 2853 cm^{-1} are characteristic of CH_2 from the curing agent. The aliphatic CH_2 also has a clear band near 1460 cm^{-1}. The band assignments of the infrared spectra from the curing agent and the epoxy resin are described elsewhere [18, 25]. It is interesting to notice that the strong band near 1510 cm^{-1} from the aromatic ring in the epoxy resin is negligible in Fig. 1A. As a result, the relatively broad band near 1613 cm^{-1} is attributed to the amino groups in the amidoamine but not to the aromatic ring because of the insignificant 1510 cm^{-1}. The presence of the amidoamine curing agent on the iron oxide also results in a clear broad amide I band appears at 1653 cm^{-1}. The absence of the bands from the epoxy resin in Fig. 1A implies that the iron oxide coated by using the solution containing 0.05 mass% epoxy system is covered mostly with the amidoamine curing agent.

The preference of the amidoamine on the iron oxide can also be easily observed by comparing the differences among Figs 1A, 1B and 1C. As shown in the spectra, the intensities of the sharp bands near 1510 and 1610 cm^{-1}, characteristic bands from the epoxy resin, increase in the order of Fig. 1C>Fig. 1B>>Fig. 1A. The intensities of

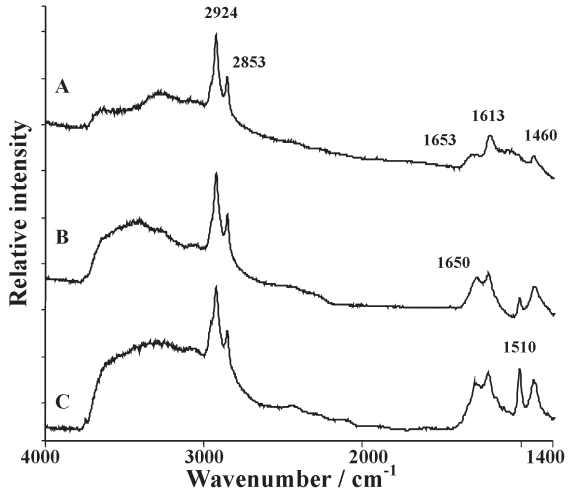

Fig. 1 The representative DRIFT difference spectra taken from the iron oxide coated in solutions containing A – 0.05 (ΔK=0.045), B – 0.2 (ΔK=0.070) and C – 1 mass% (ΔK=0.080) epoxy system

the full spectra (ΔK) also follow the same order. ΔK is the intensity of the band in the Kubelka–Munk unit. It is evident that the more the coating system on the iron oxide is, the more the epoxy molecules are present. When the amount of the coating material decreases to a certain level as in the case of Fig. 1A, a resin layer consisting of almost only the amidoamines is present on the iron oxide surface and this confirms the preferential adsorption behavior of the iron oxide. A similar behavior was found on the iron oxide hydrate and it was attributed to the acid-base reaction between the iron oxides and the amino functional groups [17].

Furthermore, the employed iron oxide also shows a special preference to the specific functional groups. It is clear that the intensities of the amide groups near 1650 cm^{-1} increase in the order of Fig. 1C>Fig. 1B>>Fig. 1A. The amino band at 1613 cm^{-1} has a smaller increase in intensity than the 1650 cm^{-1} band and becomes sharper in Fig. 1C because of the overlap with the aromatic ring near 1610 cm^{-1}. The band near 1613 cm^{-1} may also come from the contribution of the iron oxide since the hydroxyl groups on the iron oxides also exhibit a small and broad absorption band near 1620 cm^{-1}. However, this can be ignored because in the DRIFT difference spectra the baseline spectrum of the KBr powder mixed with the uncoated oxide is subtracted. It can be obtained from Fig. 1 that the intensity ratios of ΔK (1650 cm^{-1})/ΔK (1610 cm^{-1}) from Figs 1B and 1C are much greater than that from Fig. 1A. Since the contributions from the epoxy and iron oxide are neglected, the band near 1613 cm^{-1} in Fig. 1A is mainly from the amino groups. This substantiates the fact that the closer to the iron oxide surface is the more amino groups than amide groups are adsorbed onto the iron oxide surface. This seems to be consistent with the earlier study, which reported that the adsorptive sites for the amidoamine curing agent on the iron oxide were the amino and imidazoline linkages while the amide groups were inactive [17]. However, the preference of the specific functional group on the iron surface

may vary with the type of the iron substrate used and the thickness of the coating layer analyzed [16, 18].

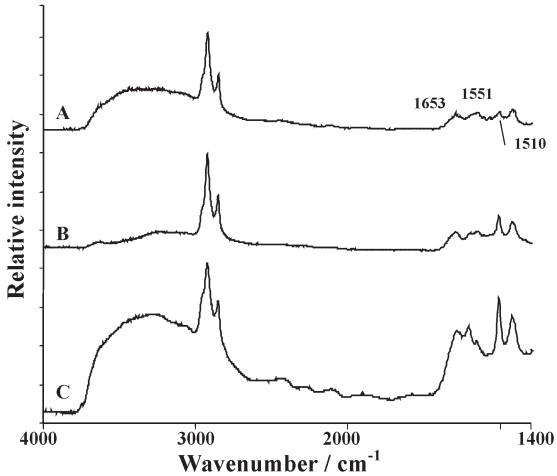

Fig. 2 The representative DRIFT difference spectra taken from the zinc oxide coated in solutions containing A – 0.05 (ΔK=0.045), B – 0.2 (ΔK=0.080) and C – 1 mass% (ΔK=0.110) epoxy system

In the case of the zinc oxide, a different adsorption behavior is obtained. Figure 2 shows DRIFT spectra taken from the zinc oxide coated with different epoxy solutions. From the spectrum shown in Fig. 2A, the bands characteristic of CH_2, 2924, 2853 and 1460 cm^{-1}, as observed in Fig. 1 are also identified. Different from that of Fig. 1A, a small band near 1510 cm^{-1} from the aromatic rings is obtained in Fig. 2A which implies the presence of the epoxy resin. In addition, no broad band near 1610 cm^{-1} as shown in Fig. 1A is observed. Nonetheless, the bands due to amide groups, the amide I band at 1653 cm^{-1} and the amide II band near 1551 cm^{-1}, are clearly shown in Fig. 2A. These amide bands also have greater intensities than 1510 cm^{-1}. These observations indicate that a lot of amide-abundant curing agents accompanying a small amount of epoxy resins are adsorbed onto the surface of zinc oxide. Unlike that on the iron oxide, the presence of amine-abundant curing agent is not significant on the zinc oxide.

A distribution of the curing agent in the resin layer on the zinc oxide surface can also be confirmed by comparing the DRIFT spectra shown in Fig. 2. As seen in the spectra, the relative intensities of the bands near 1510 and 1610 cm^{-1}, both characteristic of the aromatic ring in the epoxy, increase in the order of Fig. 2A<Fig. 2B<Fig. 2C. This trend is similar to that obtained from Fig. 1 and implies that the content of the epoxy resin increases with the coating thickness. This also confirms that the curing agent is selectively attracted to the zinc oxide surface.

The adsorption of amino compounds on the zinc oxide surface has been studied by other investigators. For example, pyridine could strongly be adsorbed onto the

acid zinc surface [26]. The result from RAIR spectra of the adsorbed pyridine suggests that pyridine is bound to strong surface Lewis acid sites on the zinc surface [27–29]. The acid-base attraction is responsible for the preferential adsorption happening on the zinc oxide [26–30]. The adsorption of ammonia on ZnO is also resulted from such an attraction [30]. In spite of the acid-base interaction, the zinc surface can react with a common latent curing agent, dicyandiamide, and then can be reduced to a carbodiimide compound [6, 31]. The described behaviors of zinc surface play an important role in determining the durability of the polymeric coatings on the galvanized steel [14, 15].

Different from those obtained on the iron and zinc oxides, a relatively weak adsorption is observed on the aluminum oxide. The DRIFT spectra from the aluminum oxide that covered with different amounts of epoxy system are shown in Fig. 3. As shown in Fig. 3A, although the characteristic bands of CH_2 (2924 and 2853 cm^{-1}) are present, their intensities are much lower than those from Figs 1A and 2A. This implies that the aluminum oxide has a smaller amount of adsorbed curing agent than the iron and zinc oxides. Furthermore, the adsorption of epoxy resin can be confirmed from the appearance of the band near 1510 cm^{-1}. The broad band above 3000 cm^{-1} is attributed to the OH groups general present on the aluminum oxide. The presence of the curing agent also results in a small broad hump near 1530 cm^{-1}, which is assigned to the amide band from the curing agent.

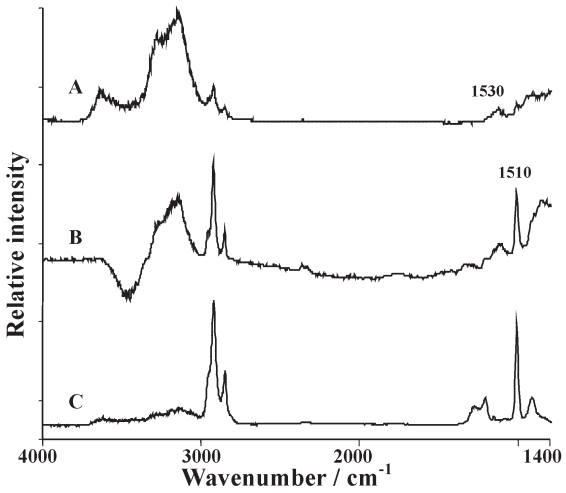

Fig. 3 The representative DRIFT difference spectra taken from the aluminum oxide coated in solutions containing A – 0.05 (ΔK=0.018), B – 0.2 (ΔK=0.020) and C – 1 mass% (ΔK=0.025) epoxy system

The relative concentrations of the resins adsorbed can also be obtained in Fig. 3. The increase in thickness of the adsorbed layer is confirmed by an increase in intensity of the spectrum from ΔK=0.018 in Fig. 3A to ΔK=0.025 in Fig. 3C. Additionally, from the intensities of the aromatic bands near 1510 cm^{-1} shown in Figs 3A, 3B, and

3C, it can be concluded that the amount of epoxy resin in the coating also increases with the coating thickness. This result is similar to those of the iron and zinc oxides. The surfaces of three metal oxides all have specific preference to the amidoamine curing agent.

The adsorption behavior of the aluminum surface is attributed to the surface acid and basic reactions as previously stated [19, 32]. This is described in other studies that studying the adsorption of amino groups onto the aluminum surface [17–19, 32]. The ion exchange reaction between the oxidized aluminum surface and the amino group can easily proceed and builds the acid-base reaction of the type $N^{+}H_3 \ldots O^{-}Al$ [19]. Both active acidic and basic sites are found to be present on the aluminum surface and the acidic sites such as aluminum ions can then attract basic molecules [19, 32].

It is well known that the experimental conditions used in DRIFT measurement, such as particle size, compression method, mechanical force applied on the powder surface, angles of incidence and collection, and the overlayer of the KBr powder, should be carefully controlled and be reproduced to obtain a meaningful qualitative result from the DRIFT spectra [33–37]. In this study, all the sampling procedures are carefully performed to minimize human error. Although the particle size of the iron oxide is smaller than that of the aluminum oxide and the zinc oxide in this study, the difference is not great and the semi-qualitative comparison made here is still informative [38].

From the previous analyses, it is concluded that three metal oxides can attract abundant curing agents onto the surface. By comparing the intensities of the DRIFT spectra, the difference in the degree of adsorption among specimens can be obtained. The ΔK of the DRIFT spectra shown in Figs 1A, 2A and 3A are 0.045, 0.045 and 0.018, respectively. This implies that the iron oxide and zinc oxide adsorb more res-

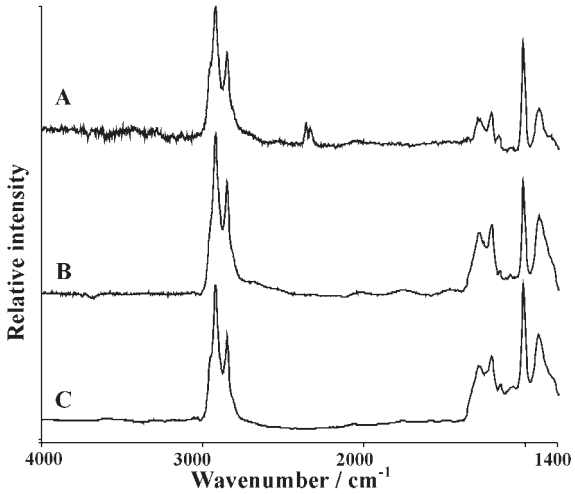

Fig. 4 The representative DRIFT difference spectra taken from A – the aluminum oxide (ΔK=0.035), B – the iron oxide (ΔK=0.095), and C – zinc oxide (ΔK=0.130) coated in epoxy system with no THF solvent

ins and adsorb more firmly than the aluminum oxide since the spectra are taken from the specimens after being rinsed with the solvent. A similar result can be obtained from spectra of the specimens with a thicker resin layer. Furthermore, from the lack of aromatic band near 1510 cm^{-1} in Fig. 1A but the appearance of this band in Figs 2A and 3A, it can be concluded that the amount of the curing agent near the oxide surface follows the order of aluminum oxide<zinc oxide<iron oxide. This can also be confirmed by the increase in intensity of the band at 1510 cm^{-1}, following the order of Fig. 3C>Fig. 2C>Fig. 1C.

Since the adsorption of polymeric resin onto the metal surface in dilute polymer solution may be different from that in solventless polymer solution, in this study the adsorption experiment is done again using the amidoamine/epoxy mixture only (no solvent) to verify the tendency of adsorption. The DRIFT spectra obtained are shown in Fig. 4. From the magnitude of ΔK, the result that the aluminum oxide attracts less resins and less firmly than the iron and zinc oxides can be confirmed. The abundance in curing agent adsorbed following the order of iron oxide>zinc oxide>aluminum oxide is also derived by the intensity ratio of ΔK (1650 cm^{-1})/ΔK (1510 cm^{-1}) following the order of Fig. 4B>Fig. 4C>Fig. 4A. As a result, the trend of the preferential adsorption obtained in the solventless epoxy mixture is similar to that in the dilute solution.

The preferential adsorption could result in a thin polymer layer adjacent to the metal surface with imbalance stoichiometry of the reactive functional groups, henceforth, generate a layer with a different curing kinetics and even with a low crosslinking density near the metal surface [1, 13, 14]. In the followings, the curing kinetics of the epoxy system filled with three metal oxides is shown. The difference in the curing reactions is detected and is related to the preferential adsorption obtained from the DRIFT spectra.

DSC analyses

The representative curing exotherms of four specimens during the DSC dynamic scan are shown in Fig. 5. The curing heats obtained from the exotherms are listed in Ta-

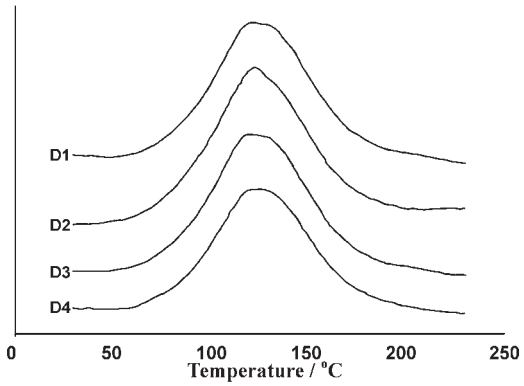

Fig. 5 The representative DSC exotherms of specimens cured at a heating rate of 10°C min^{-1}

ble 2. The heat values are in the range of 113.5–118.2 and 90.4–96.9 kJ mol^{-1} from the exotherms taken at rates of 2 and 10°C min^{-1}, respectively. It is clear that the evolved heat decreases with increasing the scanning rate for all specimens. A change in curing exotherms in the DSC dynamic measurement was found in other dynamic DSC studies [39]. The various competitive temperature-dependent curing reactions, which respond differently in the amidoamine cured epoxy system by varying the scanning rate, are responsible for the changes observed [39].

Table 2 The exotherms and glass transition temperatures of the specimens after DSC dynamic scanning measurement

Specimen		Heating rate	
		2°C min^{-1}	10°C min^{-1}
D1	ΔH/kJ mol^{-1}	113.5 (1.8)	90.4 (2.3)
	T_g/°C	77.0 (0.4)	69.0 (0.2)
D2	ΔH/kJ mol^{-1}	112.7 (0.5)	96.9 (0.7)
	T_g/°C	75.3 (1.2)	67.6 (0.2)
D3	ΔH/kJ mol^{-1}	111.9 (2.8)	91.9 (1.3)
	T_g/°C	75.38 (0.9)	67.9 (0.2)
D4	ΔH/kJ mol^{-1}	118.2 (1.4)	91.2 (1.3)
	T_g/°C	75.0 (1.1)	67.6 (0.4)

(Standard deviation); T_g – glass transition temperature

The effect of metal oxides on the exotherms can be confirmed from the heat values obtained at two different scanning rates. The specimen with no metal oxide has heat values near 113.5 and 90.4 kJ mol^{-1} from DSC exotherms taken at 2 and 10°C min^{-1}, respectively. As shown in Table 2, the specimen with the zinc oxide has the greatest heat at 2°C min^{-1} while the specimen with the iron oxide has the greatest heat at 10°C min^{-1}. The difference obtained has a high confidence level when the standard deviations of the data are considered. It is proposed that the metal oxide can affect the competitive curing mechanisms by changing the relative amounts of the functional groups near the metal surface. Henceforth, the affected curing routes respond differently to the scanning condition because of the kinetic effect inherited in the dynamic scanning measurement. The origin of this influence is attributed to the difference in the preferential adsorption confirmed in the previous DRIFT analyses. The different exotherms obtained is an indication of the changing kinetics of various curing mechanisms due to the influence of the metal oxides. This is demonstrated by the deconvoluted exotherms obtained below.

It is clear in Fig. 5 that there are two major exothermic peaks; one at a lower temperature due to the reaction of epoxy and amine while the other peak is mainly from the reaction of epoxy with the amide functional group [40]. The epoxy resin cured with an amidoamine curing agent usually contains the reaction of epoxides with the primary/secondary amines, and the reaction with the amide and the resulted alcohol [40]. In addition, the shape of exotherm from the specimen with the iron oxide is different from those of other specimens. While the specimens D1 and D3 have a similar

shape of exotherm. It is also interesting to notice that although the specimen with the zinc oxide has a similar heat value (91.2 kJ mol^{-1}) with those from the specimens D1 (90.4 kJ mol^{-1}) and D3 (91.9 kJ mol^{-1}), the exotherm of which has a different shape from those of D1 and D3. A similar conclusion can be drawn from the exotherms acquired at 2°C min^{-1}. The result here is consistent with that from the DRIFT analyses in which the specimens with the zinc and iron oxides have a more significant adsorption effect than the specimen with the aluminum oxide.

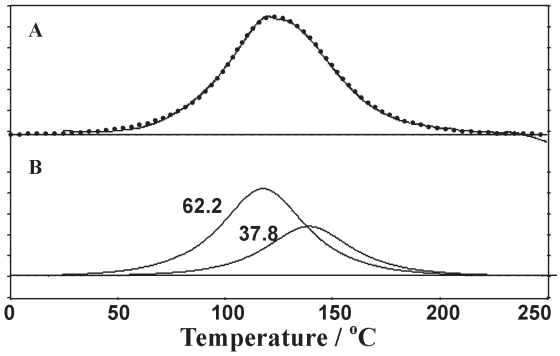

Fig. 6 The representative curve-fitted peaks calculated from the exotherm of the specimen D3 cured at a heating rate of 10°C min^{-1} A – --- original exotherm, ••• peak-fitted composite curve, and B – two peak-fitted separate curves

The difference in exotherms can also be easily identified by curve fitting method, from which two individual peaks in each curing exotherm can be separated (see representative curve-fitting spectra shown in Fig. 6). Table 3 lists the relative intensities of two deconvoluted peaks from each exotherm. Firstly, it is observed that the reaction happening at a lower temperature contains a much greater portion than the reaction at a higher temperature especially at 2°C min^{-1} regardless of the type of the specimens tested. This indicates that the amine-epoxy reaction dominates at the lower scanning speed and the reaction of epoxy/amide or epoxy/alcohol becomes more prominent at a higher scanning rate used in the DSC measurement. This is attributed to the kinetic effect on the competitive reaction mechanisms with different activation energies during the dynamic scanning process [39, 41–44].

As expected, the relative intensities of the two fitted curves are clearly different among specimens. For example, from the data taken at a rate of 10°C min^{-1} the curing exotherms of specimens D1 and D3 contain the epoxy/amine reaction about 62%. The presence of aluminum oxides shows little effect on the curing reactions. However, the addition of iron oxides in the epoxy results in an increase of the amount of amine/epoxy reaction from 62.1 to 66.5% (Table 3). But the percentage of amine/epoxy reaction decreases from 62.1 to 56.0% when the zinc oxides are present. The intensity of the epoxy/amine reaction follows the order of D2>D1~D3>D4 while the intensity of the second reaction is in the reverse order. A similar trend is also observed

from the data taken at 2°C min^{-1}. This is a clear indication of the influence of metal oxides on the curing reaction.

Table 3 The positions and relative areas of the fitted peaks from the DSC exotherms

2°C min^{-1}	Peak1 T_p/°C	Peak2 T_p/°C	Peak1 area/%	Peak2 area/%
D1	90.9 (0.2)	110.6 (1.7)	79.6 (0.6)	20.4 (0.9)
D2	87.3 (0.8)	106.8 (0.8)	83.5 (0.2)	16.5 (2.4)
D3	88.8 (0.5)	107.8 (0.8)	80.6 (1.0)	19.4 (1.7)
D4	87.0 (0.8)	108.7 (1.7)	75.1 (1.2)	24.9 (1.2)
10°C min^{-1}	Peak1 T_p/°C	Peak2 T_p/°C	Peak1 area/%	Peak2 area/%
D1	117.9 (0.2)	139.3 (0.3)	62.1 (1.6)	37.9 (1.5)
D2	118.4 (0.2)	139.9 (0.5)	66.5 (0.8)	33.5 (0.5)
D3	117.9 (0.1)	138.5 (0.2)	62.2 (1.4)	37.8 (1.5)
D4	118.4 (0.4)	139.6 (0.8)	56.0 (0.4)	44.0 (0.4)

(Standard deviation); T_p – peak temperature

The difference in relative amounts of released heats is an indication of the variation of curing reactions among specimens. In general, the existence of the metal oxide can interfere the collision probability and the proton donating capability of the curing agent with the epoxy resin and then affect complex curing mechanisms during the cure but which is believed to be only partly responsible for the change observed. Since by comparing to that from the unfilled specimen, neither evolved heat nor relative percentage of two fitted exotherms is changed in the specimen with aluminum oxide. The significant change is only obtained from the specimens with iron or zinc oxides. This is consistent with the extent of adsorption observed in the previous DRIFT analyses.

The abundant curing agent adsorbed onto the iron and zinc oxides can generate a layer of resin adjacent to the oxide surface with imbalance stoichiometry, henceforth, affect the competitive curing routes. As indicated in the introduction section, many investigators have shown that the preferential adsorption happening on the metal oxide surface can change the curing reaction of the epoxy resin and subsequently affect the resin structure and properties of the cured system because of an imbalance functionality [1, 13–16, 20, 21]. Although few changes in glass transition temperatures among specimens are obtained in this case (Table 2), the preferential adsorption of curing agent could play an important role in changing exotherms and also the kinetics of different curing mechanisms.

The kinetic characteristics of the curing reactions can be obtained by analyzing the curve fitted exotherms shown previously. For qualitative comparison, the following equation can be used to derive the curing kinetic parameters by assuming the curing reaction to be the n^{th} order reaction [45]:

$$\ln\left[\frac{1}{\Delta H_0}\left(\frac{\mathrm{d}H(t,T)}{\mathrm{d}t}\right)\right]=\ln A-\frac{E}{RT}+n\left\{\ln\left[\frac{\Delta H_0-H(t,T)}{\Delta H_0}\right]\right\}$$

where $\mathrm{d}H(t,T)/\mathrm{d}t$ is the heat release rate at the certain time t and temperature T, and ΔH_0 is the total heat released. A is the frequency factor, E is the activation energy, n is the reaction order, and R is the gas constant. As shown, the equation is of the form:

$$Z=a+bX+cY$$

As a result, the kinetic parameters A, E, and n can be calculated from the dynamic scanning exotherm by using a multiple regression method [45]. In this study, the separated peaks are analyzed with an n^{th} model kinetics. The activation energy E, the frequency factor $\ln A$, and the reaction order n calculated from 2 and 10°C min^{-1} dynamic scanning exotherms are shown in Tables 4 and 5, respectively. It is evident that the parameters calculated from the exotherms obtained at 2°C min^{-1} are slightly different than those obtained at 10°C min^{-1}. This discrepancy is caused by the kinetic effect and the simplified equation used in the dynamic scanning method and discussed by other investigators previously [41–44].

Table 4 The kinetic parameters obtained from specimens cured at a heating rate of 2°C min^{-1}

2°C min^{-1}		Peak1	Peak2
D1	n	1.26 (0.01)	1.25 (0.01)
	E/kJ mol^{-1}	56.7 (1.6)	64.3 (2.6)
	$\ln A$/1 min^{-1}	13.6 (0.6)	16.2 (0.7)
D2	n	1.20 (0.01)	1.24 (0.01)
	E/kJ mol^{-1}	53.2 (1.4)	58.9 (2.2)
	$\ln A$/1 min^{-1}	13.4 (0.4)	16.8 (0.7)
D3	n	1.25 (0.03)	1.28 (0.01)
	E/kJ mol^{-1}	54.1 (1.2)	63.4 (1.3)
	$\ln A$/1 min^{-1}	13.7 (0.4)	16.8 (0.5)
D4	n	1.25 (0.01)	1.26 (0.02)
	E/kJ mol^{-1}	51.1 (1.5)	60.7 (2.1)
	$\ln A$/1 min^{-1}	12.7 (0.5)	13.9 (0.7)

(Standard deviation)

From Table 4, the amine/epoxy reaction in specimen D1 has E near 56.7 kJ mol^{-1}, $\ln A$ about 13.6, and n near 1.26. While E, $\ln A$, and n from the proposed amide/epoxy reaction in D1 are about 64.3, 16.2 and 1.25 kJ mol^{-1}, respectively. These values are similar to those obtained by other investigators [46, 47]. In addition, it is interesting to note that although the kinetic parameters obtained from four specimens seem to be similar, the specimen D2 has the smallest n among specimens regardless of the amine or amide related reactions. Moreover, the activation energy obtained follows the order of D1>D3> D2>D4 for the epoxy/amine reaction but in the order of D1~D3>D4>D2 for the epoxy/amide reaction when the standard deviations are considered. This implies that the presence of metal oxides can affect the curing mechanisms of the epoxy/amidoamine

system [2, 6]. The most significant changes are again derived from the specimens with iron and zinc oxides. This is consistent with the previous result from the peak-fitted exotherms.

Table 5 The kinetic parameters obtained from specimens cured at a heating rate of 10°C min^{-1}

10°C min^{-1}		Peak1	Peak2
D1	n	1.28 (0.03)	1.29 (0.02)
	E/kJ mol^{-1}	57.0 (2.2)	67.3 (3.2)
	ln$A$/1 min^{-1}	13.6 (0.7)	16.0 (1.0)
D2	n	1.24 (0.01)	1.23 (0.03)
	E/kJ mol^{-1}	50.6 (0.7)	56.9 (0.4)
	ln$A$/1 min^{-1}	13.7 (1.0)	13.2 (0.5)
D3	n	1.27 (0.01)	1.26 (0.01)
	E/kJ mol^{-1}	54.3 (1.2)	61.8 (1.5)
	ln$A$/1 min^{-1}	12.4 (0.6)	13.6 (0.8)
D4	n	1.29 (0.02)	1.28 (0.02)
	E/kJ mol^{-1}	53.9 (0.9)	60.2 (1.7)
	ln$A$/1 min^{-1}	13.7 (1.0)	15.0 (1.4)

(Standard deviation)

A similar comparison can be obtained from Table 5. The reaction order n of the specimen D2 is still the smallest among those of the specimens. The activation energy obtained now follows the order of D1>D3~D4>D2 for both the epoxy/amine and the epoxy/amide reactions when the standard deviations are considered. By comparing to those from Table 4, this result indicates that the curing kinetics obtained from the dynamic measurement are varied with respect to the dynamic curing condition used in the presence of metal oxides. However, the pronounced changes are still from the specimens with iron and zinc oxides. As explained earlier, it is believed that the observed differences in curing characteristics are closely related to the effect of the preferential adsorption.

Conclusions

The curing and preferential adsorption behaviors of an epoxy/amidoamine system in the presence of iron, aluminum, and zinc oxides are shown. From adsorption bands in DRIFT spectra, it is confirmed that the amidoamine curing agent can be preferentially adsorbed on the three metal oxide surfaces because of the possible surface acid-base interaction between the metal surface and the curing agent. The concentration of amidoamine adsorbed increases in the order of aluminum<zinc<iron oxides and which difference also results in a change of curing kinetics among three specimens. Henceforth, it is obtained from the DSC analyses that more amine related exotherms happen in the specimen with the iron oxide while more amide related exotherms happen in the zinc oxide added specimen.

References

1 W. J. van Ooij, in Industrial Adhesion Problems, Ed. D. M. Brewis and D. Briggs, Wiley-Interscience Pub., New York 1985, p. 90.
2 J. Nigro and H. Ishida, J. Appl. Polym. Sci., 38 (1989) 2191.
3 S. Yoshida and H. Ishida, J. Adhesion, 16 (1984) 217.
4 H. Kollek and W. Brockmann, Proceeding of 26th National SAMPE Symposium, 1981, p. 770.
5 R. G. Dillingham and F. J. Boerio, J. Adhesion, 24 (1987) 315.
6 R. O. Cater III, R. A. Dickie and J. W. Holubka, Polym. Mat. Sci. Eng., 58 (1988) 55.
7 R. O. Cater III, R. A. Dickie, J. W. Holubka and N. E. Lindsay, Ind. Eng. Chem. Res., 28 (1989) 48.
8 W. Brockmann, O. D. Hennemann, H. Kollek and C. Matz, Int. J. Adhes. Adhesives, 6 (1986) 115.
9 M. Anand and A. K. Srivastava, J. Appl. Polym. Sci., 51 (1994) 203.
10 W. X. Zukas, K. J. Craven and S. E. Wentworth, Surf. Interf. Analysis, 17 (1991) 530.
11 S. G. Hong and J. J. Lin, J. Appl. Polym. Sci., 59 (1996) 1597.
12 Z. Petrovic and N. Stojakovic, Polymer Composites, 9 (1988) 42.
13 W. Brockmann, in Durability of Structural Adhesives, Ed. by A. J. Kinloch, Applied Science Pub., New York 1983, p.304.
14 D. J. Damico, Adhesive Age, 30 (1987) 25.
15 S. G. Hong, N. Cave and F. J. Boerio, J. Adhesion, 36 (1992) 265.
16 S. G. Hong and F. J. Boerio, J. Adhesion, 32 (1990) 67.
17 W. B. Baldwin, A. J. Milun, D. H. Wheeler and H. A. Wittcoff, J. Appl. Polym. Sci., 42 (1970) 592.
18 S. G. Hong, Angew. Makromol. Chem., 215 (1994) 161.
19 K. Nakamae, T. Nishino, X. Airu and S. Asaoka, Int. J. Adhesion and Adhesives, 15 (1995) 15.
20 J. L. Racich and J. A. Koutsky in Boundary Layers in Thermosets, Chemistry and Properties of Crosslinked Polymers, Ed. by S. Labana, Academic Press, New York 1976, p. 303.
21 F. J. Boerio and P. P. Hong, Mat. Sci. Eng., A126 (1990) 245.
22 S. G. Hong and T. C. Wang, Thermochim. Acta, 237 (1994) 305.
23 K. Horie, H. Murai and I. Mita, Fibre Sci. Tech., 9 (1976) 253.
24 H. E. Kissinger, Anal. Chem., 11 (1957) 1702.
25 S. G. Hong and H. X. Shu, J. Polym. Sci., Polym. Phys., 32 (1994) 2421.
26 F. Gaillard, E. Peillex, M. Romand, D. Verchere and H. Hocquaux, J. Surf. Interf. Anal., 23 (1995) 307.
27 E. P. Parry, J. Catal., 2 (1963) 371.
28 W. Hertl, Langmuir, 5 (1989) 96.
29 C. Morterra and G. Cerrato, Langmuir, 6 (1990) 1811.
30 M. C. Kung and H. H. Kung, Catal. Rev. Sci. Eng., 27 (1985) 425.
31 J. W. Holubka and J. C. Ball, J. Adhes. Sci. Technol., 4 (1990) 443.
32 F. Fondeur and J. L. Koenig, Appl. Spectros., 47 (1993) 1.
33 F. Boroumand, H. V. D. Bergh and J. E. Moser, Anal. Chem., 66 (1994) 2260.
34 M. P. Fuller and P. R. Griffiths, Anal. Chem., 50 (1978) 1906.
35 S. A. Yeboah, S. H. Wang and P. R. Griffiths, Appl. Spectrosc., 38 (1984) 259.
36 R. S. S. Murthy and D. E. Leyden, Anal. Chem., 58 (1986) 1228.
37 P. J. Brimmer and P. R. Griffiths, Appl. Spectrosc., 41 (1987) 791.
38 A. Tsuge, Y. Uwamino, T. Ishizuka and K. Suzuki, Appl. Spectrosc., 45 (1991) 1377.

39 R. A. Fava, Polymer, 9 (1968) 137.
40 R. B. Prime and E. Sacher, Polymer, 13 (1972) 455.
41 R. B. Prime, Polym. Sci. Eng., 13 (1973) 365.
42 H. E. Kissinger, Anal. Chem., 29 (1957) 1702.
43 E. L. Simmons and W. W. Wendlandt, Thermochim. Acta, 3 (1972) 498.
44 R. L. Reed, L. Weber and B. S. Gottfried, Ind. Eng. Chem. Fundamentals, 4 (1965) 38.
45 T. Provder, R. M. Holsworth, T. H. Grentzer and S. A. Kline, in Advances in Chemistry Series: Polymer Characterization, M. J. Comstock (Ed.), American Chemical Society, Washington, D. C., 1983, p. 233.
46 R. H. Patel and R. G. Patel, Thermochim. Acta, 160 (1990) 323.
47 I. L. Han, K. H. Hsieh and W. Y. Chiu, J. Appl. Polym. Sci., 50 (1993) 1099.